

Research Paper

Structure elucidation and antitumor activity of a new polysaccharide from Maerkang *Tricholoma matsutake*

Yiling Hou¹, Xiang Ding^{1,2✉}, Wanru Hou¹, Bo Song¹, Xianghui Yan¹

1. Key Laboratory of Southwest China Wildlife Resources Conservation, College of Life Sciences, China West Normal University, 1# Shida Road, Nanchong, Sichuan Province 637009, China
2. College of environmental science and Engineering, China West Normal University, 1# Shida Road, Nanchong, Sichuan Province 637009, China

✉ Corresponding author: E-mail: hwr@cwnu.edu.cn; Tel: 86 817 2568653. Fax: + 86 817 2568653.

© Ivyspring International Publisher. This is an open access article distributed under the terms of the Creative Commons Attribution (CC BY-NC) license (<https://creativecommons.org/licenses/by-nc/4.0/>). See <http://ivyspring.com/terms> for full terms and conditions.

Received: 2016.12.28; Accepted: 2017.05.06; Published: 2017.07.17

Abstract

A new heteropolysaccharide was isolated from the fruiting bodies of *Tricholoma matsutake* which had a molecular weight of 12078 Da. The results of structural features analysis showed that *T. matsutake* polysaccharide, here named TMP-B, was mainly composed of α -D-glucose and α -D-galactose which ratios were 7:2 and had a backbone of 1,4-linked α -D-glucose which branches were mainly composed of two 6-linked α -D-galactose residue, and the α -D-galactose was 1,6-linked. Antitumor activity results showed that heteropolysaccharide TMP-B could inhibit the growth of S180 tumor *in vivo* and promote the apoptosis of L929 cells *in vitro*. Immunoregulatory activity results showed that TMP-B could promote the proliferation of macrophages by affecting G0/G1 phase, S phases and G2/M phases and promote cytokines release and gene expression. The result of this study introduced Maerkang *T. matsutake* as a possible valuable source which helped to exhibit unique antitumor and immunoregulatory properties.

Key words: structure elucidation, biological activity, polysaccharide, Maerkang *Tricholoma matsutake*

Introduction

Polysaccharides consist of polymeric structures composed of at least ten monosaccharides sequentially connected by glycosidic bonds. Polysaccharides can be classified as homopolymers, a term used to indicate a polymer composed of identical monosaccharides, or heteropolymers, a term used for classification of polysaccharides composed of two or more types of monosaccharides. Fungal polysaccharide is a kind of active organic compounds that found in the fruiting bodies, mycelium and fermentation broth of large edible and medicinal fungi [1,2]. A large number of studies show that, fungus polysaccharide had a variety of biological activities, including anti-aging, anti-tumor, anti-oxidation, biological function and regulation of immune enhancement etc., and was recognized as the safety and low toxicity active material [3-8].

Tricholoma is a genus of fungus that contains a large number of fairly fleshy white-spored gilled

mushrooms which are found worldwide generally growing in woodlands. These are ectomycorrhizal fungi, existing in a symbiotic relationship with various species of coniferous or broad-leaved trees. The generic name derives from the Greek *trichos* meaning hair and *loma* meaning fringe or border, although only a few species (such as *T. vaccinum*) have shaggy caps which fit this description. Some well-known species are the East Asian *T. matsutake*, also known as "matsutake" or songi, and the North American species *Tricholoma magnivelare*, also known as "Ponderosa mushroom", "American matsutake", or "Pine mushroom". Some are safe to eat, yet there are a few poisonous members, such as *T. pardinum*, *T. tigrinum* and *T. equestre*. Many species originally described within *Tricholoma* have since been moved to other genera. These include the Wood blewit (*Clitocybe nuda*), previously *Tricholoma nudum*, blewit (*Clitocybe saeva*), previously *Tricholoma personatum*,

and St George's mushroom (*Calocybe gambosa*) previously *Tricholoma gambosum* [9-16].

We collected *T. matsutake* which grows in Maerkang country of Sichuan province at an elevation of 3900 m in China. In this study, a new heteropolysaccharide was obtained from the fruiting bodies of Maerkang *T. matsutake* by using DEAE-cellulose DE-52 column (Whatman (GE), New York, USA) and Sephadex G-200 column (GE, New York, USA). Its chemical structures were characterized for the first time. The structural analysis of the fraction was done by using chemical methods, IR spectroscopy, NMR spectroscopy and gas chromatography-mass spectrometry (GC-MS). The antitumor activity and immunoregulatory activity of TMP-B was evaluated. The result of this study introduced Maerkang *T. matsutake* as a possible valuable source which helped to exhibit unique antitumor and immunoregulatory properties.

Materials and methods

Materials

The fresh *T. matsutake* were collected in Maerkang country of Sichuan province, China. Maerkang country of Sichuan province in China is the locations/activities for which specific permission was not required because it is an open village of China. We also confirm that the field studies did not involve endangered or protected species because we did not go to the endangered or protected species protection zone for sampling. Following vacuum freeze-drying, the *T. matsutake* were crushed and stored at 4 °C before used in Key Laboratory of Southwest China wild Resources Conservation (Ministry of Education), College of Life Sciences, China West Normal University. Trifluoroacetic acid (TFA), 95% EtOH, KBr, standard monosaccharides, dextrans of different MWs, deuterated water, formic acid and methyl iodide were purchased from Beijing Biodee Biotechnology Co., Ltd. (Beijing, China). DEAE-cellulose DE-52 column was purchased from Whatman Co., Ltd. (Whatman (GE), New York, USA). All the other reagents used were of analytically grade.

Extraction, isolation and purification of polysaccharides from the fruiting bodies of *Tricholoma matsutake*

The fresh *T. matsutake* were dried at 60 °C and then powdered. Powdered *T. matsutake* (100g) was accurately weighed and extracted with 600 ml distilled water at 85 °C for 3h. The extractive was filtrated and centrifugated at 8000 r / min for 15 min in a high-speed centrifuge and concentrated in vacuum subsequently. Then the supernatant was added with 3 volumes of 95 % EtOH to precipitate the

crude polysaccharides (3.1g, recovery 3.1 %). The crude polysaccharides were redissolved in 100 mL of distilled water, purified with DEAE-cellulose column and was monitored by the phenol-sulfuric acid method. The elution liquid was concentrated and passed through a 6 - kDa membrane for 24 h to eliminate small molecular compounds and lyophilized. *T. matsutake* polysaccharides, named TMP-B, was obtained by vacuum freeze drying for further analysis of the structure.

Determination of molecular weight of TMP-B

The molecular weight of polysaccharide fraction was identified by high-performance gel permeation chromatography (HPGPC) (Agilent 1100 Series, Shanghai, China) [17]. An aliquot (2mg) of the dry polysaccharide was dissolved in 2 ml with double distilled water, filtered through a membrane filter (0.22 µm) and analyzed on an Agilent 1100 Series HPLC system to determine the retention time of standards and samples. The calibration curve was prepared from the standard T - series Dextran. The data were analyzed using GPC software (Millennium 32 software) (Agilent, Shanghai, China).

Fourier Transform Infrared Spectrometer (FT-IR) analysis

FT-IR spectra of the polysaccharide TMP-B were measured by grinding a mixture of polysaccharide with dry KBr, then pressing into pellets. Fourier transform infrared spectra of the TMP-B was collected using a Thermo Nicolet 6700 spectrometer (Thermo Scientific, New York, USA) operating in the range of 400 - 4000 cm⁻¹ at a resolution of 2 cm⁻¹.

Monosaccharide composition analysis of TMP-B

The polysaccharide TMP-B (2 mg) was hydrolyzed with 2 M trifluoroacetic acid (TFA) at 110°C for 6h on the mechanism of acid-catalyzed hydrolysis¹⁷. When the hydrolysis was completed, the products were dissolved with distilled water for monosaccharide composition analysis. Monosaccharide composition was measured by HPLC RID detector (Agilent HPLC 1100 Series, Shanghai, China). The operation was performed under the following conditions: a concentration of refined polysaccharide of 20 mg / ml, 75% acetonitrile as the mobile phase at 1.4 ml / min and the column oven temperature was kept at 35°C [18]. D-glucose, D-mannose, D-fructose, D-galactose, L-rhamnose, L-arabinose and D-xylose were used as standard sugars.

Atomic force micrograph (AFM)

The normal sample preparation procedure consisted of spreading of a dilute (25 µg/mL) polymer

solution onto a freshly cleaved mica surface and successive air-drying under ambient pressure, temperature, and humidity to get the dry sample. The atomic force microscopy (Bruker, Berlin, Germany) was operated in the tapping-mode.

Nuclear magnetic resonance(NMR) experiment

The polysaccharide was dissolved in deuterioxide accompanied with ultraonic wave precessing for 10 min. Then the Varian Unity INOVA 400 / 45 (Varian, New York, USA) was used to perform the ^{13}C NMR spectra and ^1H NMR spectra analysis with tetramethylsilane as internal standard.

Methylation analysis and GC-MS

The polysaccharide was methylated using methyl iodide (MeI) [19]. The completeness of methylation was confirmed by the disappearance of the hydroxyl absorption in IR spectrum in 3400 cm^{-1} . The permethylated product depolymerized with 90 % formic acid at $100\text{ }^\circ\text{C}$ for 4 h, further hydrolysed with 2 M TFA at $100\text{ }^\circ\text{C}$ for 6 h. The resulting products were derivatized using the derivatization reagent and analyzed by GC-MS (Agilent, Shanghai, China) [20, 21].

Animals

S180 tumor cells were maintained in peritoneal cavities of Kunming strain male mice obtained from Institute of Biochemistry and Molecular Immunology of North Sichuan Medical College (NSMC) (Nanchong, China). Male Kunming strain mice, weighed $25.0 \pm 1.0\text{ g}$ were housed six per plastic cages with wood chip bedding in an animal room with a 12 h light and 12 h dark cycle at room temperature ($25 \pm 2\text{ }^\circ\text{C}$) and allowed free access to standard laboratory diet. The animal experiments were conducted according to the "Guidelines for Animal Experimentation" of the North Sichuan Medical College of China which revised according to the Regulations on the administration of experimental animals of the People's Republic of China (Decree No. The second Commission of the People's Republic of China of Science and Technology Commission). We confirm that the experimental protocols were approved by the North Sichuan Medical College of China. Please see the statement including the relevant details in Supplementary Information (Guidelines for Animal Experimentation).

Assay of anti-tumor activity *in vivo*

S180 tumor cells (3×10^6) were implanted subcutaneously into right hind groin of the Kunming strain male mice. Mice were randomly divided into five groups ($n = 6$). One day after inoculation, TMP-B was dissolved in distilled water and administered

intraperitoneally (i.p.) to the mice at the doses of 20 and 40 mg/kg. Positive and negative controls were set for comparison. The positive control was given with 0.2 mL mannatide (20 mg/kg) and negative one with physiological saline instead of the test solution. Animals were sacrificed after 2 weeks. The body weights were measured. Tumors, spleens and livers were excised and the tumor inhibitory ratio were calculated by following formula: Inhibition ratio (%) = $[(A-B)/A] \times 100$, where A and B were the average tumor weights of the negative control and treated groups, respectively.

Histopathology and morphological observations

After treating the mice with TMP-B as described above, a portion of the tissues were cut into small pieces, fixed in Heidenhain's Susa Fluid (HgCl₂: 4.5 g; NaCl: 0.5 g; distilled water: 80.0 ml; formalin: 20.0 ml; acetic acid: 4.0 ml; trichloroacetic acid: 2.0 ml), and then stained with hematoxylin and eosin (HE), examined and photographed under an Olympus microscope BX53 (Olympus, Tokyo, Japan).

Immunohistochemistry preparations and morphological observations

Paraffin sections were dewaxed and hydration, repair antigen, drop sealing liquid. Add first antibody, rinse with PBS, and add biotin labeled second antibody, wash with PBS. Incubate with peroxidase solution, stain with DAB and hematoxylin, and sealed with neutral gum. Quantitative analysis of the immunohistochemistry was carried out by high resolution color graphics Image-Pro Plus 6.0 (Media Cybernetics). The positive expression color is light yellow or brown yellow, negative expression color is blue, background color is white.

Statement

The animal experiments were conducted according to the "Guidelines for Animal Experimentation" of the North Sichuan Medical College of China which revised according to the Regulations on the administration of experimental animals of the People's Republic of China (Decree No. The second Commission of the People's Republic of China of Science and Technology Commission). We confirm that the experimental protocols were approved by the North Sichuan Medical College of China. Please see the statement including the relevant details in Supplementary Information (Guidelines for Animal Experimentation).

Cell lines and reagents

The L929 cell line and RAW264.7 cell line were cultured in RPMI 1640 medium containing 10% fetal bovine serum (FBS), 1% penicillin (100 IU/mL) and

streptomycin (100 mg/L) in a humidified atmosphere with 5% CO₂ at 37 °C before use.

Pharmacological evaluation for RAW264.7 cells stimulation and L929 cells growth inhibition

The effect of TMP-B on the growth of RAW264.7 and L929 cells was determined by CCK-8-based colorimetric method, which is based on the ability of mitochondrial dehydrogenase to reduce WST-8 to the highly water-soluble orange formazan compound. Briefly, cells suspended in RPMI-1640 medium at a density of 1×10⁵ cells/well was pipetted into a 96-well plate (100µL/well) and inoculated at 37 °C in a humidified 5% CO₂ incubator for 24 h. Then, 100µL of test sample with different concentrations (0, 2.5, 5 and 10µg/mL in fresh growth medium) was added into each well separately. RPMI 1640 medium and 10 µg/mL LPS were used as the negative and positive controls, respectively. After incubation for 24 h at 37 °C, the culture medium was removed and 20 µL of CCK-8 reagent was added to each well, and the plate was further incubated for another 2-4 h. Absorbance of the colored solution at 450 nm was measured on a 96-well microplate reader (Bio-Rad, Tokyo, Japan). All experiments were performed in triplicate and the inhibitory rate was calculated as follows: Inhibition rate (%)=(1-A1/A0)×100, where A1 and A0 are the absorbance of test sample and control, respectively.

RAW264.7 cells and L929 cells cycle analysis by flow cytometry

Cells were seeded in six-well plates (5 × 10⁵ cells / well) and allowed to grow for one day before being exposed to TMP-B (2.5, 5 and 10µg/ml in fresh growth medium). 10 µg/mL LPS were used as positive controls. For cell cycle analysis, the cells were collected by trypsinization, washed twice with phosphate-buffer saline (PBS) and fixed in cold 70% ethanol for 4 h or overnight at 4°C. After an additional

wash in cold PBS, cells were resuspended in 0.5 ml of staining buffer containing 10µL RNase and 25µL propidium iodide (PI), and then incubated for 30 min in the dark at 37°C. DNA content of the cells was measured by a BD Accuri™ C6 Plus Flow Cytometer (BD, New York, USA), and the population of cells in each phase was calculated using the Modifit LT software program. For the apoptosis assay, the cells were washed twice with cold PBS, resuspended in 1×Binding Buffer, and then stained with Annexin V-FITC and PI, which were included in the Apoptosis Detection Kit (Biovision Research Products, Mountain View, CA, USA), for 30 min in the dark before being analyzed by flow cytometry. Experiments were conducted three times, and the results are reported as the mean of the three experiments.

Quantitative RT-PCR detection of related gene expression

The peritoneal macrophages were harvested after stimulated by various concentration of TMP-B for 4 h. The total cellular RNA was extracted using Trizol reagent (Invitrogen, New York, USA) and reverse-transcribed into cDNA using oligo (dT)18 primers (Invitrogen, New York, USA). Amplification of each target cDNA was performed in the iCycler system (Bio-Rad, New York, USA). PCR products were quantified using SYBR Green I. β-actin was used as an endogenous control to normalize expression levels among samples. A standard curve of each primer set was generated using LPS-induced macrophage cDNA. The PCR primers chosen were shown in Table 1. The relative expression abundance was calculated by the following formula: Relative expression abundance=mols of detected mRNA/mols of β-actin mRNA.

Cytokines determination

The analysis of cytokines was determined by an ELISA kit (R and D Systems China Co. Ltd., Shanghai, China) following the instruction of manufacturers.

Western blotting analysis

After SDS polyacrylamide gel electrophoresis of proteins extracted from RAW264.7 cells, the proteins were electrophoretically transferred to polyvinylidene fluoride(PVDF) membranes. Membranes were then blocked 2h with 5% non-fat milk in a Tris-buffered saline (TBS) containing 10mM Tris-HCl (pH 7.5) and 150mM NaCl, and then incubated with gentle shaking all the night at room temperature in the presence of the a primary antibodies: COX-2, 1:1000 dilution of purified rabbit polyclonal anti-COX-2 antibody (D5H5, CST,

Table 1. Result of primer design.

Gene	Antisense (5'-3')	Sense (5'-3')	Tm, °C	Product size, bp
β-actin	GCTGTCCCTGATGCTCT	TTGATGTCACGCACGATT	55.4	222
IL-6	GCCTTCTGGGACTGATGCTGG	CCTGGCCTTGTCTTTCITGTT	51.7	385
TNF-α	GCCTATGCTCAGCCCTCT	GGTTGACITTCCTGGTAT	53.4	423
iNOS	GAGCGAGTTGTGGATTGTC	GGGAGGAGCTGATGGAGT	55.2	376
IL-1β	GCCCATCTCTGTGACTC	CTGCTTGTGAGGTGCTGA	52.0	434
COX-2	CAGCACTTCACGCATCAGTT	AAGCGTTTGCGGTACTCATT	52.6	803

Tm, temperature; iNOS, inducible nitric oxide synthase.

Shanghai, China); iNOS, 1:1000 dilution of purified rabbit polyclonal anti-iNOS antibody (D6B6S, CST, Shanghai, China); β -Actin, 1:3000 dilution of purified rabbit polyclonal anti- β -Actin antibody (bs-0061R, Beijing Biosynthesis Biotechnology CO. LTD, Beijing, China). The blots were washed three times with TBS and incubated under gentle agitation with the secondary antibodies: COX-2 and iNOS, anti-rabbit IgG combined with conjugated with horseradish peroxidase 1: 3000 dilution (#7074, CST, Shanghai, China); β -Actin, anti-rabbit IgG combined with conjugated with horseradish peroxidase 1: 3000 dilutions (CW0103, cwbiotech, Beijing, China), at room temperature for 2 h and then washed three times with 50mM Tris-HCl (pH 7.5) buffer TBST. The blot was developed using Pro-light HRP chemiluminescent Kit (PA112, Tiangen CO. LTD, Beijing, China).

Statistical methods

All data were presented as means \pm standard deviation (SD) of three replications. Statistical

analyses were performed using student's t-test and one-way analysis of variance. * $P < 0.05$ and ** $P < 0.01$ (vs. control) were considered to be a statistically significant and very significant finding, respectively.

Results

Structure elucidation

The new polysaccharide, named TMP-B, was obtained as a water-soluble light yellow powder from the fruiting bodies of *T. matsutake*, with a yield of 3.1%. HPGPC of the polysaccharide fraction shows that each fraction was represented by a broad and symmetrical peak on the chromatograms (Figure 1A and Figure 1B) which indicate a higher purity level of TMP-B. The dextran standards were used to create a calibration curve for elucidating the molecular weights of TMP-B. The molecular weight (Mw) of TMP-B was around 16347 Da, the peak molecular weight was 12078 Da, the number-average molecular weight was 3734 Da, and the polydispersity was 4.38 (Figure 1A and Figure 1B).

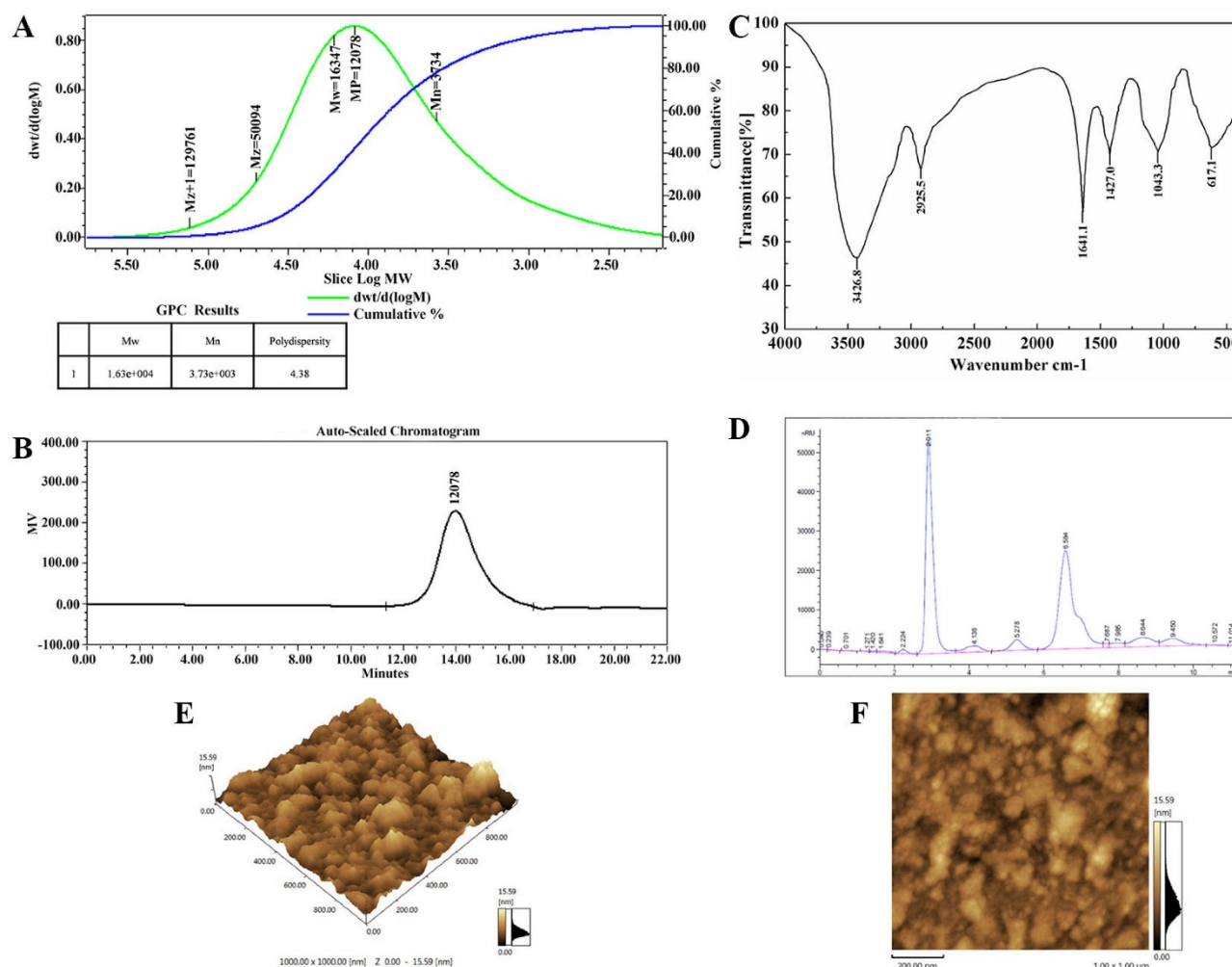


Fig. 1. (A) The high performance gel permeation chromatogram of TMP-B. (B) The molecular weight of TMP-B. (C) Fourier transform infrared spectra of TMP-B. (D) The component monosaccharides analysis of polysaccharides by HPLC. (E-F) Atomic force microscopy (AFM) cubic images of the frontside (E) and lateral sides (F) of molecular structure of polysaccharide TMP-B.

The IR spectrum of the sample (Figure 1C) showed that the absorption was very obvious in the more than 3000 cm^{-1} , which were caused by the stretching vibration and angular vibration of O-H linkage. The absorption peak at 2925.3 cm^{-1} was C-H stretching vibration absorption peak of TMP-B. The absorption band at 1629.3 cm^{-1} was caused by OH deformation vibration. The strong absorption bands at 1404.5 cm^{-1} was due to C-H bending vibration. The absorption peaks at 1045.4 cm^{-1} in the range of $1200\text{--}1000\text{ cm}^{-1}$ in the IR spectrum suggested that the monosaccharides in the two samples had a pyranose-ring. Meanwhile, the bands at 597.3 cm^{-1} was due to C-H rocking vibration.

The composition analysis of polysaccharides is an important step to control the quality and got basic information about the polysaccharides. In this study, the TMP-B polysaccharides samples was hydrolyzed with TFA and then the component monosaccharides were analyzed by HPLC with Agilent refractive index detector. Compared with the retention time of the standard monosaccharide, the peak at retention time of 6.584 min represents the α -D-glucose. In addition, there is a shoulder peak near the retention time of 6.584 min which represents the α -D-galactose. The results of structural features analysis showed that *T. matsutake* polysaccharide was mainly composed of α -D-glucose and α -D-galactose which ratios were 7:2 (Figure 1D). TMP-B was also in good agreement with the D-configuration monosaccharide according to GC-MS analysis.

The topographical AFM planar image of the dry sample of TMP-B deposited from a $25\text{ }\mu\text{g}/\text{mL}$ water solution was shown in Figure 1E and Figure 1F. Only spherical lumps could be seen and the diameter and height of the lumps ranged from 0 to 15.59 nm. The heights of the spherical structures are much higher than that of a single polysaccharide chain (about 0.1-1 nm), suggesting that molecular aggregation was involved. We can see that irregularly shaped large structures were formed together like worm from AFM cubic image of TMP-B, which suggested that TMP-B could take random coil compact conformation. The conformation might be related to its side chains.

The hydrogen spectrum of TMP-B is shown in Figure 2A. According to the integral curve of the hydrogen spectrum, the results show that the purity of TMP-B is greater than 95%. In the ^1H NMR(400HZ) spectrum, δ 5.074 and δ 4.992 indicate there were two anomeric hydrogen existing in TMP-B, suggesting that TMP-B was composed of two monosaccharides and these sugar residues are α pyranose, as the H-1 chemical shift greater than 4.95. The signals at δ 3.432- δ 4.538 are the signal peak of remaining proton which mostly formed by a number of signal peaks

overlapped. δ 4.790 was the hydrogen signal of water. The ^{13}C NMR spectrum of TMP-B (Figure 2B) showed the anomeric peaks were centralised in δ 103.05, δ 102.96 and δ 101.54 ppm, indicating there was only α anomeric configuration of monomer existing in TMP-B. The results are consistent with the analysis results of IR and ^1H NMR. The chemical shift was not found in the region between δ 160 and δ 180 ppm, indicating there were no carboxyl in TMP-B. The presence of TMP-B signal confirmed that all monomers should be pyranring, as furan ring signals should be around δ 106-109 ppm. According to the literature¹⁰, the resonances in the region of 101-104 ppm in the ^{13}C NMR (400 MHz) spectrum of TMP-B were attributed to the anomeric carbon atoms of -D-galactosepyranose (-D-Galp) and -D-glucosepyranose (-D-Glup). In the anomeric carbon region, signals at δ 102.96 could be attributed to C-1 of \rightarrow 4)- α -D-Glu-(1 \rightarrow ; δ 103.05 to C-1 of \rightarrow 3,6)- α -D-Glu-(1 \rightarrow ; δ 101.54 to C-1 of α -D-Gal-(1 \rightarrow) (Figure 2B). All the assignment of the carbon atoms signals was shown in Table 2.

Table 2. ^{13}C NMR chemical shift data (δ , ppm) for polysaccharide TMP-B.

Sugar residues	Chemical shift, δ (ppm)					
	C1	C2	C3	C4	C5	C6
\rightarrow 4)- α -D-Glcp-(1 \rightarrow)	102.96	67.26	71.83	74.65	68.04	65.20
\rightarrow 4,6)- α -D-Glcp-(1 \rightarrow)	103.05	68.35	73.42	76.00	69.54	70.47
\rightarrow 6)- α -D-Galp-(1 \rightarrow)	101.54	68.95	73.55	78.13	70.96	61.53

The methylated products of TMP-B were hydrolysed with acid, converted into silane compound, and analysis by GC-MS. Experiment data were settled and listed in Table 2. The information in MS showed that fragment ion peaks were consistent with data of D-configuration monosaccharide fragment ion peaks which can be concluded that the glucose and galactose residues were D-configuration respectively (Figure 2C-2G). You et al [10]. previously reported the structural characterisation of polysaccharides from *T. matsutake* which consisted of glucose, galactose and mannose with a molar ratio of 5.9:1.1:1.0. In our study, the methylation analysis for TMP-B proved that the α -D-glucosepyranose residues were 2, 3-bis-O-methyl-substituted and 2, 3, 6-tris-O-methyl-trisubstituted, the α -D-galactosepyranose residues were 2, 4-bis-O-methyl-substituted and 3, 4-bis-O-methyl-substituted (Figure 2C-2G and Table 3). Results methylated linkage analysis of TMP-B indicated that (1 \rightarrow 4)-linked α -D-glucosepyranose was one of the largest amounts residue of the polysaccharide structure, the branched residue was (1 \rightarrow 4, 6)-linked α -D-glucosepyranose revealing that (1 \rightarrow 4)-linked α -D-

glucosepyranose should be also possible to form the backbone structure. Residues of branch structure were terminated with α -D-galactosepyranose residues. It is concluded that a repeating unit of TMP-B has a backbone of (1 \rightarrow 4)- α -D-glucosepyranose and (1 \rightarrow 4, 6)- α -D-glucosepyranose. The branch was supposed to be the composition of one with (1 \rightarrow 6)- α -D-galactosepyranose residue.

On the basis of the above experimental data, we elucidated the possible structure of TMP-B had a backbone of 1, 4-linked- α -D-glucose and 1, 4, 6-linked- α -D-glucose which branches were mainly composed of two (1 \rightarrow 6)-linked- α -D-galactosepyranose residue (Figure 2H).

Anti-tumor activity of TMP-B

To detect the anti-tumor activity of TMP-B *in vivo*, we used the mice transplanted S180 to evaluate the effects and the results were summarized in Table 4. TMP-B could inhibit the growth of the tumors ($P < 0.01$) in a dose-dependent manner. The inhibitory rate in mice treated with 20 mg/kg TMP-B was 61.565%,

being the highest in the two doses. Furthermore, during the experiments, the appetite, activity and coat luster of each animal in TMP-B groups were better than the mice treated with mannatide. The results showed little change in average liver weight in test groups which indicating that TMP-B did not cause serious sliver damage. On the 14th day, the average tumor weight of negative control mice was 0.588 g, whereas the average tumor weight of mice in TMP-B group significantly reduced in doses of 20 mg/kg and 40 mg/kg, which were 0.226 g and 0.263 g, respectively (Figure 3A). Polysaccharide with high molecular in high concentration will lead to the aggregation of molecules, which will eventually affect the anti-tumor activity [22]. But the specific molecular mechanism needs further study. It is noteworthy that the average weights of the spleens and thymus in test groups were significantly greater in doses of 20 mg/kg than that in the mannatide mice, and even that of the negative control mice, indicating that TMP-B could increase the weights of immune organs in moderate doses.

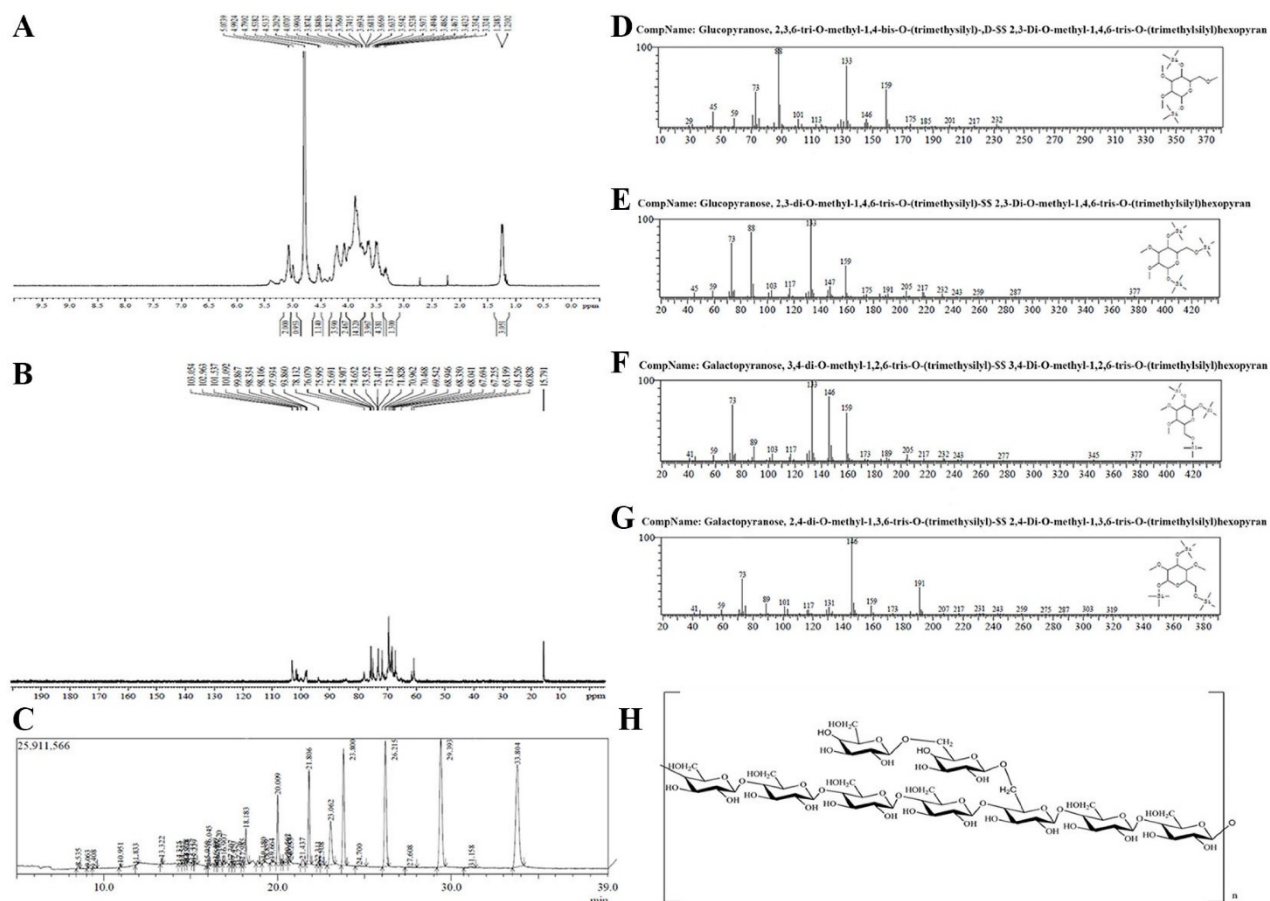


Fig. 2. (A) The ^1H NMR spectra of TMP-B. (B) The ^{13}C NMR spectra of TMP-B. (C)The GC-MS spectra of TMP-B. (D)The fragment ion peaks of 2, 3, 6-Me $_2$ -Glc. (E)The fragment ion peaks of 2, 3-Me $_2$ -Glc. (F)The fragment ion peaks of 3, 4-Me $_2$ -Galacp. (G)The fragment ion peaks of 2, 4-Me $_2$ -Galacp. (H) Predicted chemical structure of polysaccharide TMP-B.

Table 3. GC–MS results of methylation analysis of TMP-B.

Methylated sugar	Linkage	m/z
2,3,6-Me-1,4-Glu	1,4-	29 45 59 73 88 101 113 133 146 159 175 185 201 217 232
2,3-Me-1,4,6-Glu	1,4,6-	45 59 73 88 103 117 133 147 159 175 191 205 217 232 243 259 287 377
3,4-Me-1,2,6-Gal	1,6-	41 59 73 89 103 117 133 146 159 173 189 205 217 232 243 277 345 377
2,4-Me-1,3,6-Gal	1,6-	41 59 73 89 101 117 131 146 159 173 191 207 217 231 243 259 275 287 303 319

Table 4. Anti-tumor activities of TMP-B on S180 tumor (mean±SD, n=6).

Group	Spleen index (mg / g)	Liver index (mg / g)	Thymus index (mg / g)	Average tumor weight (g)	Inhibitory rate of tumor (%)
Control	4.634±0.853	48.925±2.988	1.301±0.328	0.588±0.354	
TMP-B1	3.394±0.826	46.732±2.835	1.432±0.399	0.226±0.043	61.565(**)
TMP-B2	4.809±1.205	45.655±5.442	1.365±0.322	0.263±0.046	55.272(**)
Man	3.821±0.728	49.505±1.755	1.102±0.231	0.197±0.088	66.497(**)

Significant differences from negative control group and positive control group were evaluated using Student's t test: *P < 0.05, **P < 0.01.
Control: negative control group; TMP-B1, TMP-B2 indicating TMP-B groups of 20 mg/kg and 40 mg/kg, respectively; Man: positive control group of mannate.

Histology of immune organs of liver, spleen, and thymus shows that tissues arranged more regular and firmer in TMP-B group than those in the control group and S180 group (Figure 3B). These results suggested that activating immune responses in the host might be one of the mechanisms of anti-tumor activity of TMP-B, as many anti-tumor polysaccharides found in the world.

Immunohistochemistry analysis

Immunohistochemistry (IHC) refers to the

process of detecting antigens (e.g. proteins) in cells of a tissue section by exploiting the principle of antibodies binding specifically to antigens in biological tissues. Specific molecular markers are characteristic of particular cellular events such as proliferation or cell death (apoptosis). Immunohistochemistry is widely used in basic research to understand the distribution and localization of biomarkers and differentially expressed proteins in different parts of a biological tissue [23]. The liver as a mediator of systemic and local innate immunity and an important site of immune regulation is now an accepted concept. The critical metabolic functions of the liver often eclipse any perception of its role as an immune organ. Here, we detected three immune factors that are secreted by the liver using immunohistochemistry analysis. In our experiment, the positive expression color is light yellow or brown yellow, negative expression color is blue, background color is white (Figure 4A). The results showed that COX-2, IL-1β and TNF-α were mainly expressed in cell cytoplasm, cell membrane, and stroma in liver. Statistical analysis showed a very significant increase (**P < 0.01) in the expression of IL-1β with an OD value of 0.2519 and a significant increase (*P < 0.05) in the expression of COX-2 and TNF-α in TMP-B group with an OD value of 0.1611 and 0.2594, respectively, compared with the control group. It is worth noting that the expression of these three kinds of immune factors were less than S180 group (Figure 4B-4D). The relevant mechanism need to be further studied.

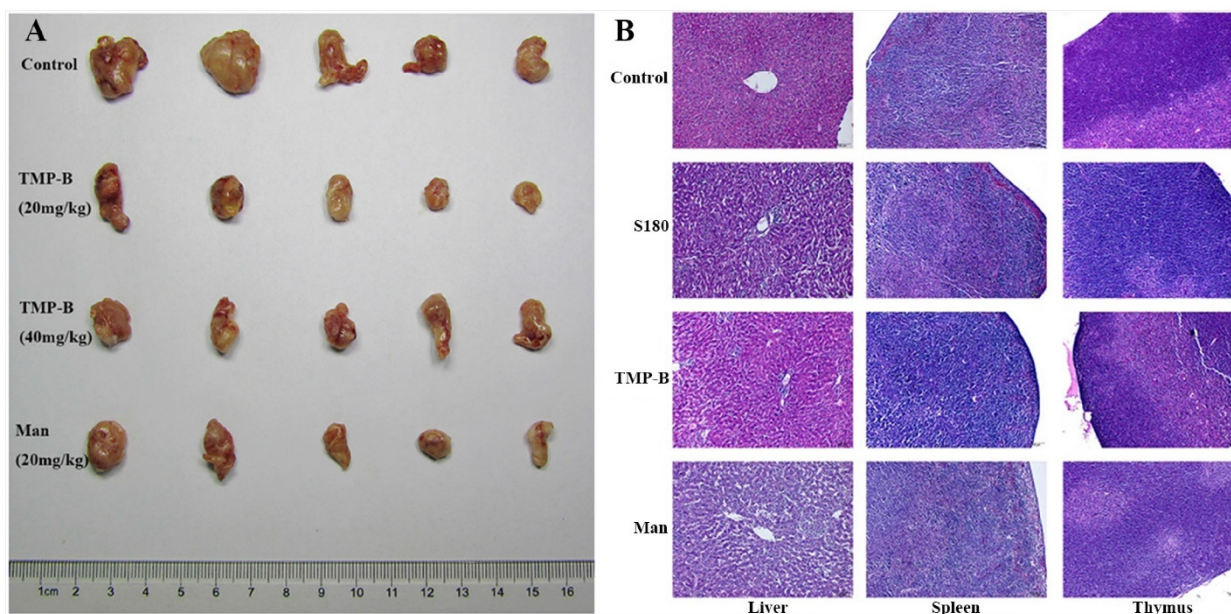


Fig. 3. (A) Anti-tumor activity of TMP-B *in vivo*. (B) Histological preparations of the liver, spleen and thymus in TMP-B group compared with control group.

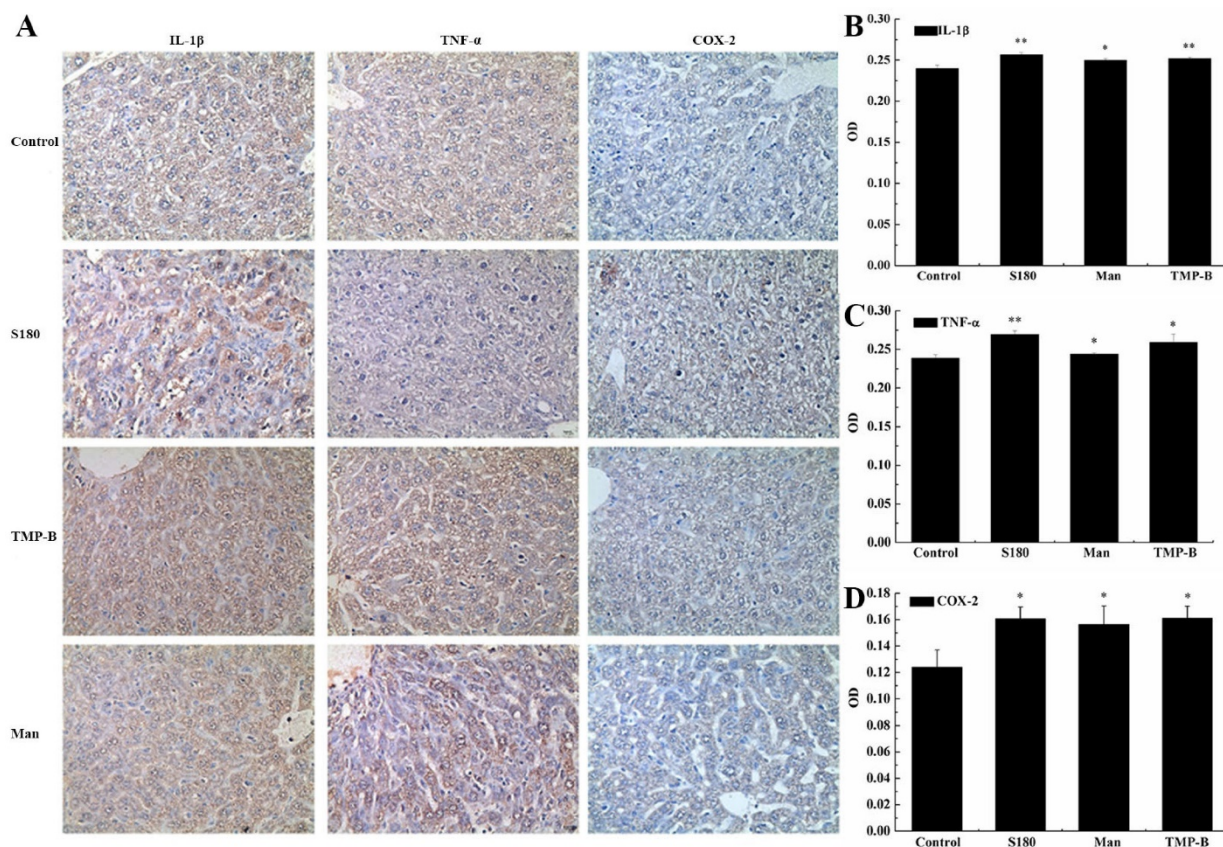


Fig. 4. (A) Immunohistochemistry preparations of the liver in TMP-B group compared with control group. Note: Control: Normal mice; S180: S180 tumor bearing mice injected with physiological saline; TMP-B: S180 tumor bearing mice injected with TMP-B (concentration of 20 mg/kg); Man: S180 tumor bearing mice injected with mannate (concentration of 20 mg/kg). (B-D) Statistical analysis of IL-1 β (B), TNF- α (C) and COX-2(D) in liver. P values are indicated as *P < 0.05 and **P < 0.01.

Effects of TMP-B on tumor cells growth and apoptosis *in vitro*

Cervical cancer L929 cells were incubated up to 24 h in the presence or absence of TMP-B at concentration of 2.5, 5 and 10 μ g/mL, and measured by CCK-8 method. The results showed that the polysaccharide TMP-B had significantly toxicity effects on Cervical cancer L929 cell line. As presented in Figure 5A and Figure 5B, the cell viability was markedly decreased after exposure to TMP-B in a dose-dependent manner. Upon a concentration of 5 and 10 μ g/mL of TMP-B, L929 cells showed a significant decrease in OD value of 0.5099 and 0.5926, respectively, (*P < 0.05) compared with the control group and LPS group. Thus, TMP-B seems to be capable of exerting inhibition effect on L929 cell proliferation.

The change in DNA content during progression of the cell cycle was also evaluated by flow cytometry. A representative example depicting the effect of TMP-B treatment for 24 h on cell cycle phase distribution is shown in Figure 5B. In the cells

undergoing apoptosis, a special DNA peak (usually called the sub-G0/G1 peak or apoptotic peak) appeared. This peak is thought to be one of the characteristics of apoptosis. As shown in Figure 5B, treatment with 2.5, 5 and 10 μ g/ml of TMP-B for 24 h resulted in the accumulation of cells in the S phase (5.3, 5.2 and 8.5%, respectively), compared with that in the LPS group (8.6%). In addition, the sub-G0/G1 apoptotic fraction was markedly increased when TMP-B was applied, compared with that in the LPS group (17.1%), treatment with 2.5, 5 and 10 μ g/ml of TMP-B for 24h resulted in the increasing of apoptotic fraction (from 11.8% to 15.2% and 19.5%, respectively). Taken together, these results demonstrated that TMP-B suppressed L929 cell proliferation by inducing apoptotic cell death, and causing S arrest.

Detection of L929 cell apoptosis by laser scanning confocal microscopy showed that the L929 cell appear chromatin condensation, marginalization, nuclear membrane lysis, and the chromatin is divided into blocks and appear apoptotic bodies (Figure 5C).

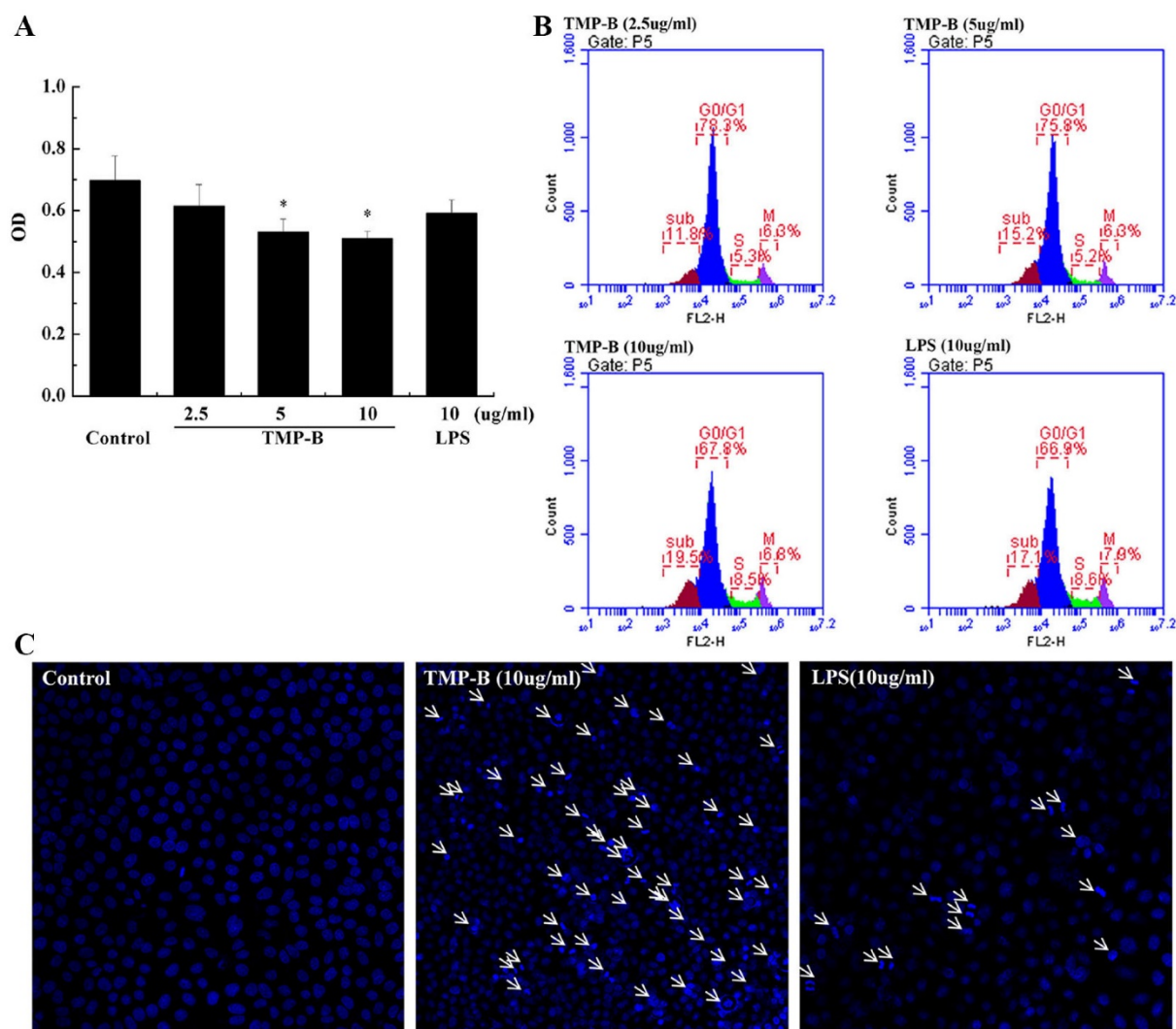


Fig. 5. (A) Inhibition rate of L929 cells following TMP-B treatment *in vitro*. (B) Effects of TMP-B on the apoptosis cell cycle distribution of L929 cells *in vitro*. (C) Morphological observation of L929 cells. The arrow indicates the apoptotic cells. P values are indicated as *P < 0.05 and **P < 0.01.

Effects of TMP-B on the proliferation and cell cycle distribution of RAW264.7 cells *in vitro*

The anti-tumor activity of the polysaccharide was usually believed to be a consequence of the stimulation of the cell-mediated immune response. Macrophages occupy a unique position in the immune system because they can initiate natural immune responses and then act as effector cells that help manage immune responses such as inflammation, angiogenesis and fighting an infection [24-27]. The results show the cell proliferation activity was lowest when the macrophages were exposed to medium alone, whereas the incubation of these cells with TMP-B showed a obvious increase in cell proliferation (Figure 6A). TMP-B (5 $\mu\text{g} / \text{ml}$, *P < 0.05; 10 $\mu\text{g} / \text{ml}$, **P < 0.01) was able to significantly promoted RAW264.7 cell proliferation compared with the control group with an OD value of 0.3733 and 0.4046, respectively. Furthermore, the cell

proliferation activity at a concentration of 10 $\mu\text{g} / \text{ml}$ TMP-B was even greater than the activity elicited by 10 $\mu\text{g} / \text{ml}$ LPS. Cell morphology observation also showed that the increases of cell volume in RAW264.7 cells.

Cell cycle analysis was performed on RAW264.7 cells using flow cytometry to examine the effects of TMP-B on cell cycle progression. Figure 6B and Figure 6C shows the effects of TMP-B on the cell cycle phase (G0/G1, S and G2/M) distribution of RAW264.7 cells using flow cytometry with PI staining. The treatment of RAW264.7 cells with TMP-B at 2.5, 5 and 10 $\mu\text{g} / \text{mL}$ for 24 h induced a decrease in the G2/M phase population from 23.03 % of the control group to 24.60 %, 24.93 % and 26.56%, respectively (*P < 0.05 or **P < 0.01), with a decrease in the percentage of cells in the G0/G1 phase from 47.23 % of the control group to 42.97%, 42.20% and 40.70%, respectively (*P < 0.05 or **P < 0.01). These results suggested that TMP-B could

promote the proliferation of macrophage cells by abolishing cell cycle arrests in the G₀/G₁ phases and promoting cell cycle progression in G₂/M phase, which might induce cell division.

Quantitative RT-PCR determination

TNF- α is a cell signaling protein (cytokine) involved in systemic inflammation and is one of the cytokines that make up the acute phase reaction. It is produced chiefly by activated macrophages, although it can be produced by many other cell types such as CD4⁺ lymphocytes, NK cells, neutrophils, mast cells, eosinophils, and neurons. IL-6 is secreted by T cells and macrophages to stimulate immune response, e.g. during infection and after trauma, especially

burns or other tissue damage leading to inflammation. Quantitative RT-PCR results showed a significant increase in the level of IL-1 β , IL-6, TNF- α , iNOS and COX-2 mRNA in TMP-B-treated (10 μ g/ml) RAW264.7 cells compared to those untreated. The positive control, LPS 10 μ g/ml, also promoted the expression of these genes. The relative expression of the genes studied (IL-1 β , IL-6, TNF- α , iNOS and COX-2) in the untreated macrophage were 0.36, 0.31, 0.92, 0.86 and 0.68, respectively, but increased dramatically to 1.23, 1.28, 6.98, 7.09 and 6.96 in a dose-dependent manner in the TMP-B-treated (10 μ g/ml) cells, respectively (Figure 7A).

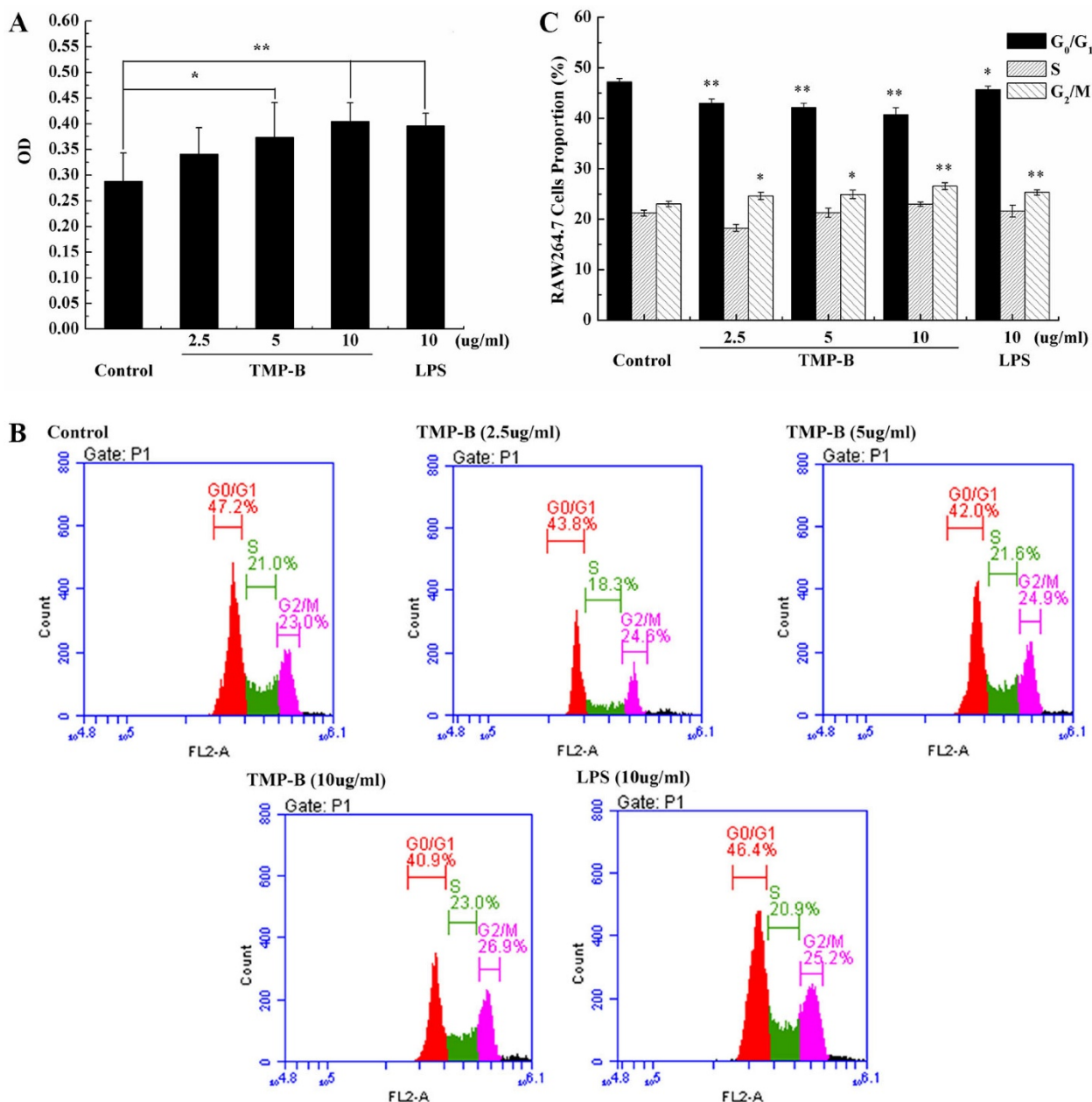


Fig. 6. (A) Proliferation activity of RAW264.7 cells following TMP-B treatment *in vitro*. (B) Effects of TMP-B on the Cell Cycle Distribution of RAW264.7 Cells *in vitro*. (C) Statistical analysis of growth cycle of RAW264.7 Cells following TMP-B treatment *in vitro*.

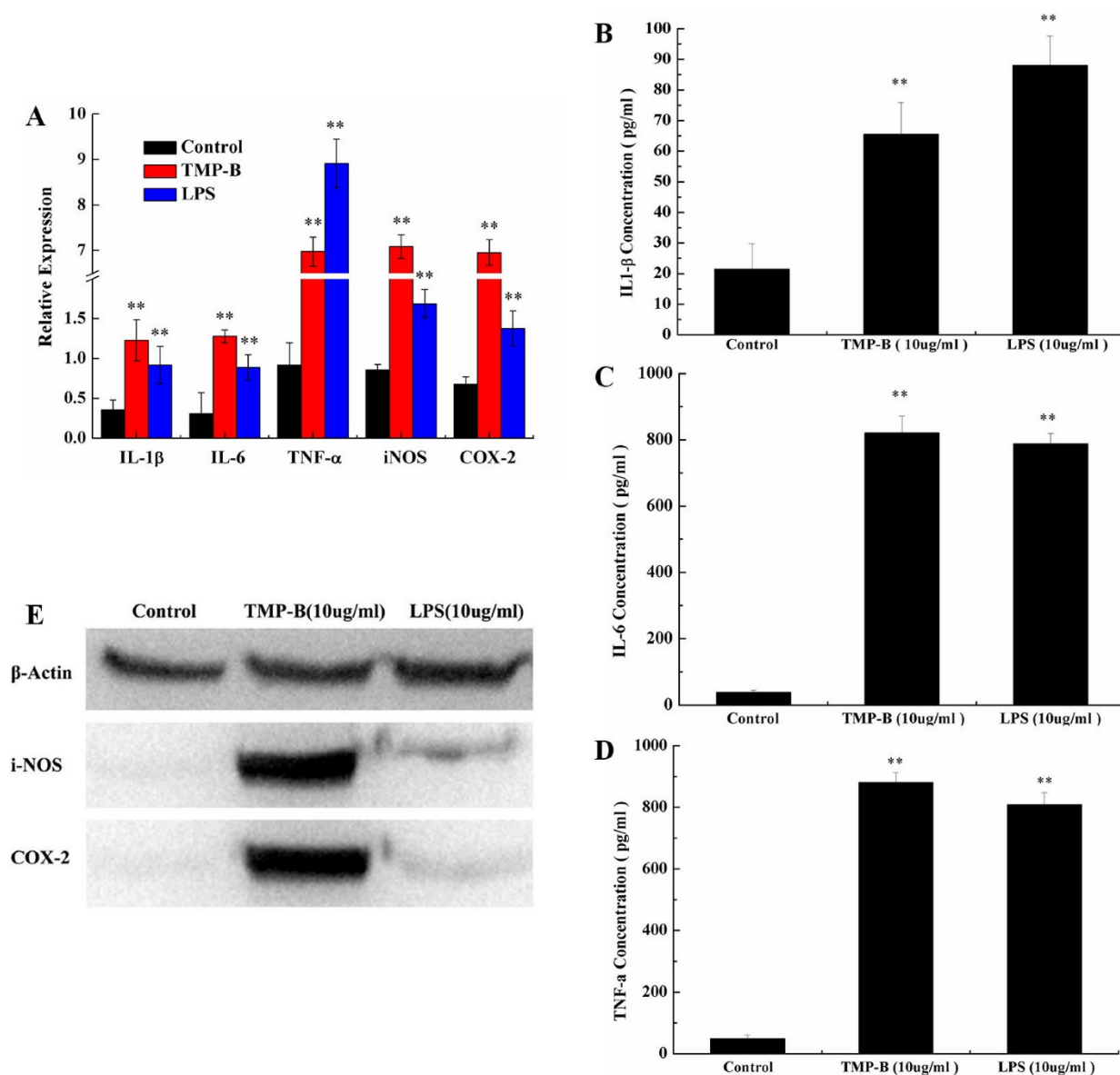


Fig. 7. (A) Expression of TNF- α , iNOS, IL-6 and IL-1 β mRNA in PM stimulated by TMP-B. Control: Negative control group; TMP-B: TMP-B group (concentration of 20 mg/kg); LPS: LPS group (concentration of 20 mg/kg). (B-D) ELISA assays of IL-1 β (B), IL-6(C) and TNF- α (D) in RAW264.7 cells *in vitro*. (E) Western Blot analysis of iNOS and COX-2 in RAW264.7 cells *in vitro*. P values are indicated as *P < 0.05 and **P < 0.01.

Cytokines determination

Phagocytes are armed with inducible nitric oxide synthase (iNOS), which is activated by interferon-gamma (IFN- γ) as a single signal or by tumor necrosis factor (TNF) along with a second signal. In this way, the immune system may regulate the armamentarium of phagocytes that play a role in inflammation and immune responses. It is also worth noting that IL-6's role as an anti-inflammatory cytokine is mediated through the effects of TNF- α , IL-1 and IL-10, et al. Obviously, the level of IL-1 β (Figure 7B), IL-6 (Figure 7C) and TNF- α (Figure 7D) secreted by TMP-B-stimulated (10 μ g / ml) macrophages was much higher than medium-treated macrophages with a concentration of 66.5429,

821.1944 and 880.3636 pg/ml, respectively. And IL-6 and TNF- α secreted even much higher than induced by LPS

Western blotting analysis

It has confirmed that COX-2 can be induced in macrophages, fibroblasts, endothelial cells and monocytes. Under physiological conditions, there was no expression of COX-2 in cells of most tissues; while in inflammation, cancer and other pathological conditions, the expression of COX-2 increased through mediators of inflammatory stimuli, damage, mitotic original and carcinogenic substance, and participate in a variety of physiological and pathological processes. The inducible isoform, iNOS, is involved in immune response, binds

calmodulin at physiologically relevant concentrations, and produces NO as an immune defense mechanism, as NO is a free radical with an unpaired electron. It is the proximate cause of septic shock and may function in autoimmune disease. The differential abundance levels of protein factors in cultured macrophages cells were confirmed by western-blot analyses for iNOS and COX-2. The western-blot analyses use the Quantity One software to analysis and the results show that the iNOS and COX-2 protein content is very low in the blank group which can hardly be detected, while both of the two protein levels increased significantly in TMP-B group (10 $\mu\text{g}/\text{ml}$) in RAW264.7 macrophages (Figure 7E). The results showed that the polysaccharides TMP-B stimulation can enhance the iNOS and COX-2 protein levels in macrophage which further strengthen the supposed immune modulatory potential of TMP-B.

Discussion

Polysaccharides are closely related to the regulation of immune function, identification of cell and cell, intercellular substance transportation, cancer diagnosis and treatment, etc. Polysaccharide is also a good adjuvant in medicine [28].

One of the most important biological activities of polysaccharides is to improve host immune function. Polysaccharides play an important role in anti-tumor effect through immune related cells, including B lymphocytes, T lymphocytes, dendritic fine cells, macrophages and natural killer cells (NK) [29]. The results showed that polysaccharide TMP-B can activate RAW264.7 cell, and the activated immune cells can regulate many bioactive substances, such as interleukin -1β (IL- 1β), tumor necrosis factor alpha (TNF- α) and interleukin -6 (IL-6), which play an important role in the anti-tumor immunity. TMP-B could also promote the proliferation of macrophage cells by abolishing cell cycle arrests in the G0/G1 phases and promoting cell cycle progression in G2/M phase, which might induce cell division. The results indicated the polysaccharides TMP-B may play the anti-tumor role by activating macrophage function. The relevant mechanism need to be further studied, including the anticancer target that the polysaccharide is acting on and the signal transduction pathways.

The pharmacological activity of polysaccharide largely depends on its structure characteristics, such as molecular weight, solubility, viscosity, primary structure and advanced structure [30].

There were significant differences in antitumor activity of polysaccharides with different monosaccharide composition. Glucose is the basic structural unit of many polysaccharides. In addition to glucose, the polysaccharide which also has a certain

antitumor activity is mainly composed of galactose (Gal), mannose (Man), arabinose (Ara), rhamnose (Rha), xylose (Xyl), etc [31, 32]. The structure of TMP-B composed of α -D-glucose and α -D-galactose which ratios were 7:2 showed the basic structure of antitumor activity.

The main chain structure of polysaccharide is also an important factor to determine the antitumor activity of polysaccharides, which includes two aspects: the type of glycosides bond and the configuration of the main chain. Generally speaking, the polysaccharides with the structure of β -helix have higher activities. For example, the β -(1 \rightarrow 3)-D dextran has the higher activities than that of α -(1 \rightarrow 3)-D dextran [33]. At the same time, the composition of branched chain and molecular weight also have a great influence on the antitumor activity of polysaccharides, which may be related to the higher configuration of polysaccharide molecules. The activity of polysaccharides with moderate degree of branching (DB) and molecular weight tended to be higher. It is difficult to achieve the ideal activity with too large or too small of DB and molecular weight. Each polysaccharide has its own most suitable DB and molecular weight [34,35]. The new heteropolysaccharide from the fruiting bodies of *T. matsutake* had a molecular weight of 12078 Da which is in the best relative molecular mass range.

The activity of some polysaccharides was closely related to the chemical groups. These chemical groups can be added and removed by artificial chemical reactions. Therefore, the structural modification of polysaccharide can improve the activity of polysaccharide. It is possible to affect the activity of polysaccharide by means of the following factors, such as sulfation, carboxymethylation, methylation, hydroxyethylation [36]. For example, the number and position of the acetyl groups in polysaccharide had a great influence on the activity of polysaccharide. The toxicity of polysaccharide will be reduced or disappeared after structural modification. After carboxymethylation, the activity of Mannan obtained from will retain while it's toxicity will disappear [37].

The premise of polysaccharide to exert its antitumor activity is that it can be dissolved in water. The water solubility of polysaccharide was increased and its pharmacological activity was also improved accordingly. Therefore, it is possible to enhance the antitumor activity of water soluble polysaccharides by proper chemical modification of increasing solubility [38,39]. It is reported that after partial carboxymethylation, both the water solubility and the anti tumor activity of the water insoluble β -(1 \rightarrow 3)-D dextran increased. The new heteropolysaccharide TMP-B has a certain water solubility and has a

backbone of 1, 4 - linked α - D - glucose which branches were mainly composed of two 6 - linked α - D - galactose residue, and the α - D - galactose k, was 1, 6 - linked. Although it had the structure of α -(1 \rightarrow 4)-D glucose, the molecular weight of the heteropolysaccharide was moderate and this may lead to high antitumor activity.

Acknowledgements

This project was supported by National Natural Science Foundation of China (31400016 and 31200012), the Science and Technology Support Project of Sichuan Province (2014SZ0020 and 2014FZ0024), the Cultivate Major Projects of Sichuan Province (14CZ0016 and 16CZ0018), and the Open Foundation of Microbial Resources and Drug Development of Key Laboratory of Guizhou Province (GZMRD-2014-002).

Author Contributions

Y. H. and X. D. conceived and designed the experiments. Y. H., X. D., W. H. and B. S. performed the experiments. Y. H., X. D., W. H., B. S. and X. Y. analyzed the data. Y. H. and X. D. wrote the manuscript. All authors discussed the results and commented on the manuscript.

Competing Interests

The authors have declared that no competing interest exists.

References

- Hibbett DS, Binder M, Bischoff JF, et al. A higher level phylogenetic classification of the fungi. *Mycol Res.* 2007; 111: 509-547.
- Bertozzi CR, Kiessling LL. Chemical glycoobiology. *Science.* 2001; 291: 2357-2364.
- Bittencourt VC, Figueiredo RT, Dasilva RB, et al. An alpha-glucan of *Pseudallescheria boydii* is involved in fungal phagocytosis and toll-like receptor activation. *J Boil Chem.* 2006; 281: 22614-22623.
- Borchers AT, Stern JS, Hackman RM, et al. Mushrooms, tumors, immunity. *P Soc Exp Biol Med.* 1999; 221: 281-293.
- Pauline MR, Time E, Peter C, et al. Glycosylation and the immune system. *Science.* 2001; 291: 2370-2376.
- Brown GD, Herre J, Williams DL, et al. Dectin-1 mediates the biological effects of beta-glucans. *J Exp Med.* 2003; 197: 1119-1124.
- Angeli JP, Ribeiro LR, Gonzaga ML, et al. Protective effects of β -glucan extracted from *Agaricus brasiliensis* against chemically induced DNA damage in human lymphocytes. *Cell Boil Toxicol.* 2006; 22: 285-291.
- Cordero RJ, Frases S, Guimaraes AJ, et al. Evidence for branching in cryptococcal capsular polysaccharides and consequences on its biological activity. *Mol Microbiol.* 2011; 79: 1101-1117.
- Cho IH, Choi HK, Kim YS. Comparison of umami-taste active components in the pileus and stipe of pine-mushrooms (*Tricholoma matsutake* Sing.) of different grades. *Food Chem.* 2010; 118: 804-807.
- Lijun Y, Qing G, Mengying F, et al. Structural characterisation of polysaccharides from *Tricholoma matsutake* and their antioxidant and antitumour activities. *Food Chem.* 2013; 138: 2242-2249.
- Yuji T, Hayato M. Structure and expression of two phenylalanine ammonia-lyase genes of the basidiomycete mushroom *Tricholoma matsutake*. *Mycoscience.* 2015; 56: 503-511.
- Yang S, Ren X, Sheng J, et al. Preparation and the antitumor activity *in vitro* of polysaccharides from *Tricholoma matsutake*. *World J Microb Biot.* 2010; 26: 497-503.
- Youngeon K, Jiwon Y, Changho L, et al. ABTS Radical Scavenging and Anti-Tumor Effects of *Tricholoma matsutake* Sing. (Pine Mushroom). *J Korean Soc Food Sci Nutri.* 2009; 38: 463-468.
- Ishihara Y, Iijima H, Yagi Y, et al. Enhanced recovery of NK cell activity in mice under restraint stress by the administration of a biological response modifier derived from the mycelia of the basidiomycete *Tricholoma matsutake*. *Stress.* 2003; 6: 141-148.
- Liu G, Wang H, Zhou B, et al. Compositional analysis and nutritional studies of *Tricholoma matsutake* collected from Southwest China. *J Med Plants Res.* 2010; 4: 1222-1227.
- Liu G, Wang H, Luo Y, et al. Simultaneous determination of 6 active components in traditional Chinese medicine "KANGXIN" tablets by RP-HPLC-DAD. *J Med Plants Res.* 2010; 4: 298-303.
- Yu RM, Yin Y, Yang W, et al. Structural elucidation and biological activity of a novel polysaccharide by alkaline extraction from cultured *Cordyceps militaris*. *Carbohydr Polym.* 2009; 75: 166-171.
- Fan YJ, He XJ, Zhou SD, et al. Composition analysis and antioxidant activity of polysaccharide from *Dendrobium denneanum*. *Int J Boil Macromol.* 2009; 45: 169-173.
- Sun Y, Liu J. Purification, structure and immunobiological activity of a water-soluble polysaccharide from the fruiting body of *Pleurotus ostreatus*. *Bioresource Techn.* 2009; 100: 983-986.
- Yiling H, Lu L, Xiang D, et al. Structure elucidation, proliferation effect on macrophage and its mechanism of a new heteropolysaccharide from *Lactarius deliciosus* Gray. *Carbohydr Polym.* 2016; 152: 648-657.
- Ding X, Hou Y, Hou W. Structure elucidation and antioxidant activity of a novel polysaccharide isolated from *Boletus speciosus* Forst. *Int J Boil Macromol.* 2012; 50: 613-618.
- Durand, A. Aqueous solutions of amphiphilic polysaccharides: Concentration and temperature effect on viscosity. *Eur Polym J.* 2007; 43: 1744-1753.
- Yun X, Qaiser C, Christopher S, et al. Bioconjugated quantum dots for multiplexed and quantitative immunohistochemistry. *Nat Protoc.* 2007; 2: 1152-1165.
- Gordon S, Martinez FO. Alternative activation of macrophages: mechanism and functions. *Immunity.* 2010; 32: 593-604.
- Martinez FO, Helming L, Gordon S. Alternative activation of macrophages: an immunologic functional perspective. *Annu Rev Immunol.* 2009; 27: 451-483.
- Gordon S. Alternative activation of macrophages. *Nat Rev Immunol.* 2003; 3: 23-35.
- Lawrence T, Natoli G. Transcriptional regulation of macrophage polarization: enabling diversity with identity. *Nat Rev Immunol.* 2011; 11: 750-761.
- Wasser SP. Medicinal mushrooms as a source of antitumor and immunomodulating polysaccharides. *Appl Microbiol Biot.* 2002; 60: 258-274.
- Guo L, Xie J, Ruan Y, et al. Polysaccharides PS-G and protein LZ-8 from Reishi (*Ganoderma lucidum*) exhibit diverse functions in regulating murine macrophages and T lymphocytes. *J Agr Food Chem.* 2010; 58: 8535-8544.
- Schepetkin IA, Quinn MT. Botanical polysaccharides: Macrophage immunomodulation and therapeutic potential. *Int Immunopharmacol.* 2006; 6: 317-333.
- Gan L, Zhang SH, Yang XL, et al. Immunomodulation and antitumor activity by a polysaccharide-protein complex from *Lycium barbarum*. *Int Immunopharmacol.* 2004; 4: 563-569.
- Moretao MP, Zampronio AR, Gorin P AJ, et al. Induction of secretory and tumoricidal activities in peritoneal macrophages activated by an acidic heteropolysaccharide (ARAG-AL) from the gum of *Anadenanthera colubrina* (Angico branco). *Immunol Lett.* 2004; 93: 189-197.
- Ukawa Y, Ito H, Hisamatsu M, et al. Antitumor effects of (1 \rightarrow 3)- β -D-glucan and (1 \rightarrow 6)- β -D-glucan purified from newly cultivated mushroom *hatakeshimaji* (*Lyophyllum decastes* Sing.). *J Biosci Bioen.* 2000; 90: 98-104.
- Yang JH, Du YM, Huang RH, et al. Chemical modification and antitumor activity of Chinese lacquer polysaccharide from lac tree *Rhus vernicifera*. *Carbohydr Polym.* 2005; 59: 101-107.
- Surenjav U, Zhang LN, Xu XJ, et al. Effects of molecular structure on antitumor activities of (1 \rightarrow 3)- β -D glucans from different *Lentinus Edodes*. *Carbohydr Polym.* 2006; 63: 97-104.
- Wang YF, Zhang LN, Li YQ, et al. Correlation of structure to antitumor activities of five derivatives of a β -glucan from *Poria cocos sclerotium*. *Carbohydr Res.* 2004; 339: 2567-2574.
- Tao YZ, Zhang LN, Cheung PCK. Physicochemical properties and antitumor activities of water-soluble native and sulfated hyperbranched mushroom polysaccharides. *Carbohydr Res.* 2006; 341: 2261-2269.
- Bohn JA, Bemiller JN. (1 \rightarrow 3)- β -D Glucans as biological response modifiers: a review of structure-functional activity relationships. *Carbohydr Polym.* 1995; 28: 3-14.
- Unursaikhan S, Xu XJ, Zeng FB, et al. Antitumor activities of O-sulfonated derivatives of (1 \rightarrow 3)- α -D glucan from different *Lentinus edodes*. *Biosci Biotech Bioch.* 2006; 70: 38-46.